JOURNAL OF ELECTROMAGNETIC ENGINEERING AND SCIENCE, VOL. 19, NO. 2, 115~121, APR. 2019

https://doi.org/10.26866/jees.2019.19.2.115
ISSN 2234-8395 (Online) · ISSN 2234-8409 (Print)

Effects of Split Position on the Performance of a Compact Broadband Printed Dipole Antenna with Split-Ring Resonators

Kam Eucharist Kedze · Heesu Wang · Ikmo Park*

Abstract

This paper presents the effects of the position of the split of a split-ring resonator (SRR) on the performance of a composite broadband printed dipole antenna. The antenna is made of two printed dipole arms enclosed by two rectangular and identically printed SRRs. One dipole arm and the SRR are printed on the top side of the substrate, while the other dipole arm and SRR are printed on the bottom side of the same substrate. By changing the position of the split on the SRR, different antenna characteristic values are obtained, namely, for impedance bandwidth and radiation patterns. The split position is thus a critical parameter in antenna design, because it influences the antenna's major performance immensely. Different split positions and their consequences for antenna performance are demonstrated and discussed. The antenna generates linearly polarized radiations, and it is computationally characterized for broadband characteristics. The optimized compact antenna has overall dimensions of 9.6 mm × 74.4 mm × 0.508 mm (0.06λ × 0.469λ × 0.0032λ at 1.895 GHz) with a measured fractional bandwidth of 60.31% (1.32 to 2.46 GHz for $|S_{11}| < -10$ dB) and a radiation efficiency of >88%.

Key Words: Broadband, Compact Size, Composite Antenna, Dipole Antenna, Split Ring Resonator (SRR).

I. Introduction

Split-ring resonators (SRRs) have been widely used to meet the design requirements of broadband capability, low profile, and compactness for electrically small antennas (ESAs) [1–6]. SRRs are generally made of two metallic concentric and coupled rings with slits on opposite ends. This specific configuration was proposed by Pendry et al. [7] to build up for the negative permeability medium. An SRR can be either a thin metallic ring or a square loop with a split on a dielectric substrate. SRRs are one of the first metamaterial-based microwave resonators, and their geometries are much smaller than the wavelength of the exciting electromagnetic wave [8]. Recently, SRRs have gained significance in the design of ESAs. Their ability and potential to produce strong electromagnetic resonances have made them an outstanding solution in antenna miniaturization [9]. SRRs are practicable in bandwidth enhancement, with their ability to couple strongly to other resonant elements. Antennas incorporated with SRRs for bandwidth improvements can exhibit diverse antenna performance characteristics depending on the configuration and position of the split in the SRRs [10–15].

In this paper, we present the effects of SRR position on the performance of a compact broadband antenna with omnidirectional radiation patterns that is composed of a printed dipole

Manuscript received September 18, 2018 ; Revised December 22, 2018 ; Accepted January 11, 2019. (ID No. 20180918-067J)
Department of Electrical and Computer Engineering, Ajou University, Suwon, Korea.
*Corresponding Author: Ikmo Park (e-mail: ipark@ajou.ac.kr)

and two rectangular SRRs. The proposed antenna demonstrates a broad impedance-matching bandwidth by generating multi-resonances. The number of resonances and, consequently, the bandwidth are adjustable, and they can be reallocated by altering the SRR split position. Therefore, the SRR introduces certain variations into the antenna performance as a function of the SRR split position. By moving the SRR split position along the lengths of the SRR, different antenna characteristics can be demonstrated. Then the performance characteristics of the composite antenna in different split positions are analyzed computationally with the aid of the ANSYS HFSS software.

II. Antenna Geometry and Performance

The proposed composite antenna configuration of the printed dipole with SRRs is shown in Fig. 1 [16]. The dipole is printed on the top and bottom sides of a thin Rogers RO5880 dielectric substrate ($\varepsilon_r = 2.2$, $\tan\delta = 0.0009$, and $h = 0.508$ mm). On both sides of the same substrate, two SRRs are placed to encompass each arm of the dipoles. The SRR splits are located on opposite sides of the origin of each SRR. Excitation is done by a coaxial feed with the characteristic impedance of 50 Ω. The outer conductor of the coaxial line is connected to the bottom arm of the dipole, and the inner conductor of the coaxial line extends through the substrate and connects to the top arm of the dipole [17–19]. The optimized design parameters of the antenna for a wide impedance bandwidth and omnidirectional radiation patterns are as follows: $e = 17.3$ mm, $W_l = 9.6$ mm, gap = 3 mm, $L_d = 34.7$ mm, $W_d = 3.7$ mm, $h = 0.508$ mm, $W_s = 2$ mm, $G_{p1} = G_{p2} = 12.2$ mm, $L_s = 74.4$ mm, and $L_l = 54.5$ mm.

To achieve compact lightweight broadband antennas with good and non-deteriorating radiation patterns, two SRRs are coupled to a half-wavelength dipole to generate multi-resonances [20]. The SRRs are designed to encircle each dipole arm in order to increase the area of interaction between the dipole and SRR, thereby ensuring strong coupling. However, the SRR split position is a crucial and sensitive design parameter that requires an optimum position for effective operation of the antenna. The SRR split position influences the performance of the antenna in a number of ways, such as (1) the coupling between the dipole and SRRs, (2) the number of generated resonant modes, (3) the impedance bandwidth, and (4) the radiation patterns.

When the SRR splits are not properly positioned on both SRRs, the SRRs do not couple to the dipole; therefore, the antenna does not resonate. For instance, as shown in Fig. 2, no resonance is noted or identified when the SRR split position becomes $G_{p1} = G_{p2} = 34.2$ mm. The SRRs do not couple to the dipole, causing the dipole not to resonate in this configuration.

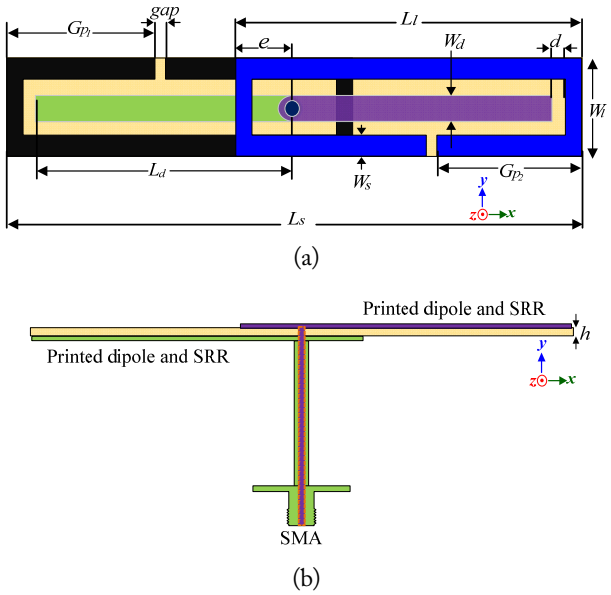

Fig. 1. Geometry of the printed dipole loaded with SRRs: (a) top view and (b) side view [16].

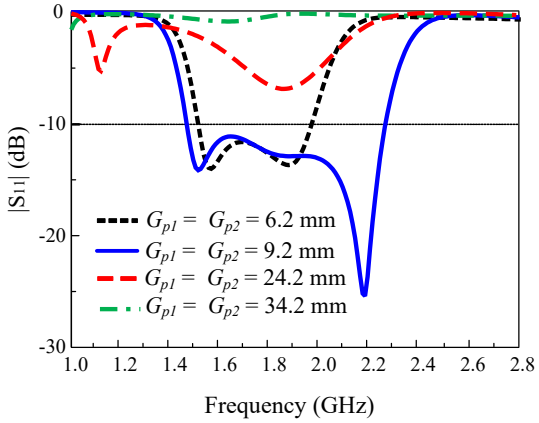

Fig. 2. Reflection coefficient of the dipole antenna loaded with SRRs for different SRR split positions.

Fig. 2 also illustrates the result of the configuration when $G_{p1} = G_{p2} = 24.2$ mm. In this case, the dipole is excited and generates a single resonance. However, the SRRs are weakly coupled to the dipole, and so they produce an almost negligible resonance.

By altering G_{p1} and G_{p2} to 6.2 mm, the SRR couples to the dipole effectively and generates two resonances, as shown in Fig. 2. The first resonance in this configuration is generated by the full lengths of both SRRs, which are operating as arms of a dipole to resonate at a low frequency. The second resonance is generated by the dipole element. These two resonances interact to provide an appreciable impedance bandwidth for the antenna.

It is also worth mentioning that at a split position of less than 6.2 mm, the antenna responds in a similar fashion to its response at 6.2 mm by producing two resonant modes. Meanwhile, at a split position greater than 34.2 mm, the antenna remains unexcited, as in the case of a 34.2 mm split position.

When $G_{p1} = G_{p2} = 9.2$ mm, a third resonant mode appears at a high frequency. This resonance increases the bandwidth of the antenna significantly. The third resonance at a high frequency is generated from the overlapping area of the SRRs. The overlapping portion becomes excited at a high frequency and resonates at a half wavelength, consequently enhancing the antenna impedance bandwidth, as shown in Fig. 2. This demonstrates that retaining the same antenna structure but changing the SRR split position results in a significant bandwidth improvement of the antenna.

As another example of the effects of the SRR split position, Fig. 3 shows the antenna reflection coefficient when the SRR split positions are at $G_{p1} = 2.7$ mm and $G_{p2} = 17.2$ mm. In this particular configuration, the antenna produces the widest possible impedance bandwidth by generating four resonant modes.

The previous antenna configuration included the three resonant modes described above. However, a fourth resonance is introduced around the third resonance frequency; consequently, it pushes the third resonance slightly to the higher frequency for a further bandwidth improvement with a fractional bandwidth of about 55.47%.

This configuration produces a wide bandwidth but suffers from antenna radiation pattern distortions with high cross polarization at 2.24 GHz, as shown in Fig. 4. The radiation pattern is tilted slightly in one direction in both the xz- and xy-planes. The gain curve in this configuration experiences a dip, as shown in Fig. 5.

Accordingly, to eliminate the dip in gain and the poor radiation performance in the radiation pattern of the previous antenna configuration, while nonetheless maintaining the broad impedance bandwidth of the antenna, the SRR split positions need to be located at a symmetrical position near the center of both SRRs. When $G_{p1} = G_{p2} = 12.2$ mm, the antenna generates good performance features.

The optimized antenna configuration generates broadband

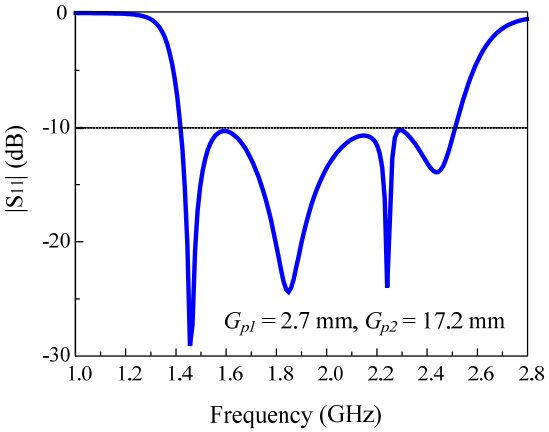

Fig. 3. Reflection coefficient of the dipole antenna loaded with SRRs for $G_{p1} = 2.7$ mm and $G_{p2} = 17.2$ mm.

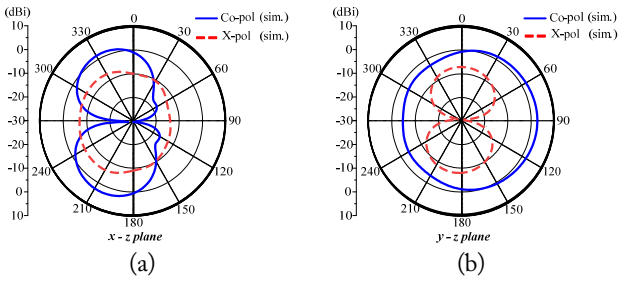

Fig. 4. Radiation pattern of the dipole antenna loaded with SRRs for $G_{p1} = 2.7$ mm and $G_{p2} = 17.2$ mm at 2.24 GHz: (a) xz-plane and (b) yz-plane.

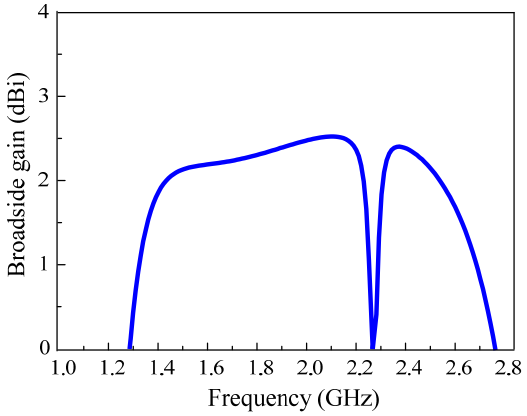

Fig. 5. Broadside gain of the dipole antenna loaded with SRRs for $G_{p1} = 2.7$ mm and $G_{p2} = 17.2$ mm.

characteristics, with the bandwidth covering 1.38 to 2.41 GHz, which is the fractional bandwidth of 54.35%. The overall dimensions of the antenna are 9.6 mm × 74.4 mm × 0.508 mm (0.06λ × 0.469λ × 0.0032λ at 1.895 GHz). The antenna produces good radiation patterns and gain curves without any significant loss of impedance bandwidth, as compared to the configuration with four resonances.

As illustrated in Fig. 6, the antenna generates three resonances. The first resonance resulted from the full lengths of the

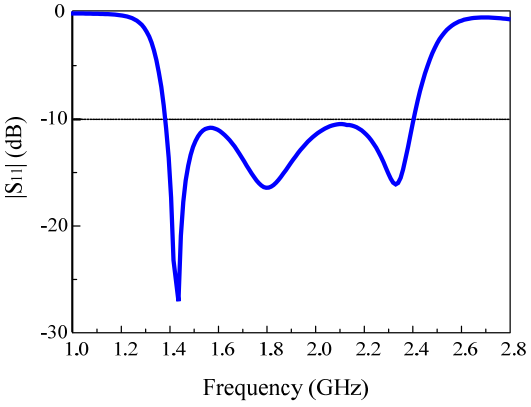

Fig. 6. Reflection coefficient of the optimized dipole antenna loaded with SRRs.

SRRs oscillating in unison as a half-wavelength dipole. This resonance occurs at a low frequency of the antenna. The intermediate resonance is generated by the dipole, while the third resonance at a high frequency is a consequence of the SRR being excited partially in the overlapping area of the SRRs. In this mode, just the overlapping portion of the SRRs resonates at a half wavelength. Interactions between these resonances produce a wide impedance bandwidth for the antenna.

The split position contributes immensely to antenna bandwidth improvement, but in contrast, the size of the split has little consequence on the impedance bandwidth, as shown in Fig. 7. The figure illustrates the effect of the SRR split size on the reflection coefficient of the antenna.

As the split size increases, the effective length of the SRR decreases and causes a shift in the low-frequency resonance to the right of the reflection coefficient curve. On the other hand, when the split size decreases, the effective length of the SRR increases; this results in a shift to the left in the reflection coefficient profile. The split size affects only the low-frequency resonance, because the changes in the split size have no impact on the dipole and overlapping area of the SRRs, which are responsible for the other resonances. This further validates the view that the SRR split position is critical to antenna design, as compared to its size.

The optimized antenna produces a stable gain with insignificant fluctuations within its impedance bandwidth. Fig. 8 shows the gain variations of the antennas as frequency changes. The dip, which occurred in the gain curve of the antenna configuration with a fourth resonance, has now been eliminated. The antenna is linearly polarized with low levels of cross polarization within the impedance bandwidth.

Fig. 9 shows the radiation patterns of the antenna at three frequency points. The radiation patterns are symmetric and dipole-like, with less variation and deterioration within the impedance bandwidth.

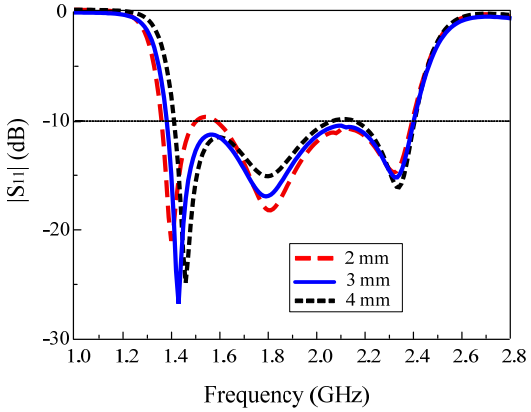

Fig. 7. Reflection coefficient values of the dipole antenna loaded with SRRs for different SRR split sizes (gap).

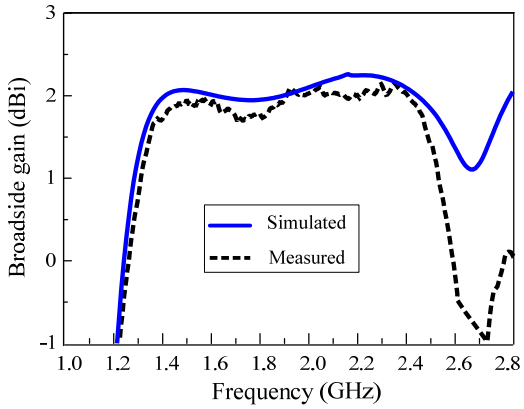

Fig. 8. Simulated and measured broadside gain of the optimized dipole antenna loaded with SRRs.

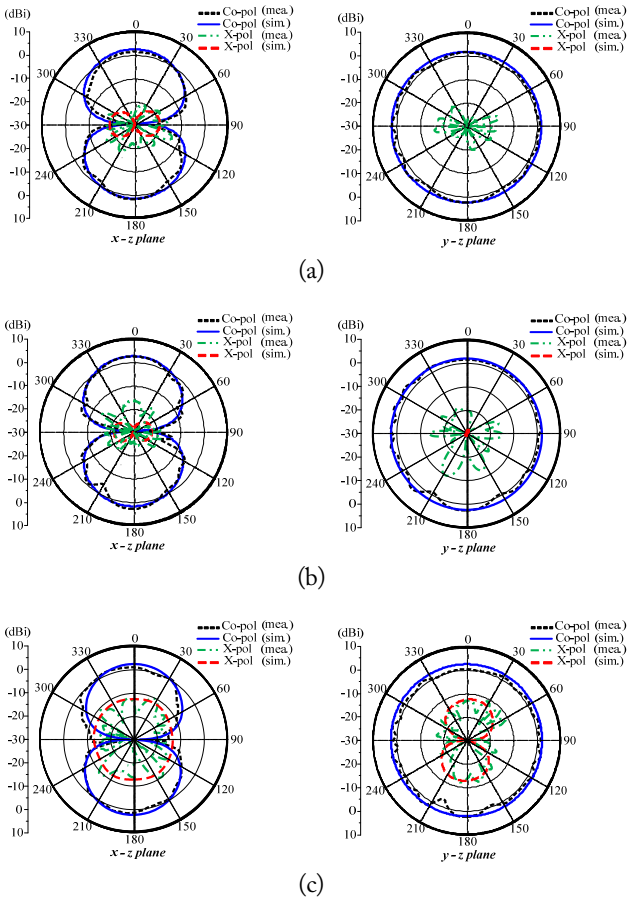

Fig. 9. Measured and simulated radiation patterns of the optimized dipole antenna loaded with SRRs at 1.42 GHz (a), 1.8 GHz (b), and 2.33 GHz (c) [16].

III. Experimental Results

Fig. 10 shows the proposed antenna fabricated with a balun to eliminate common mode current and generate clean symmetric radiation patterns. With overall dimensions of 9.6 mm × 74.4 mm × 0.508 mm (0.06λ × 0.469λ × 0.0032λ at 1.895 GHz), the antenna demonstrated broad impedance bandwidth.

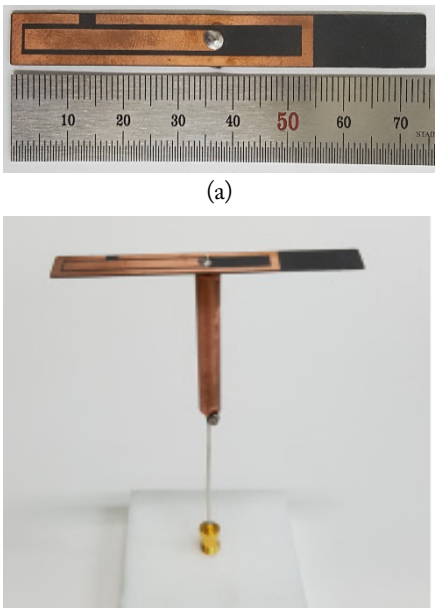

(a)

(b)

Fig. 10. Fabricated sample of the proposed antenna with a balun: (a) top view and (b) perspective view [16].

The prototype's reflection coefficient was measured using an Agilent N5230A network analyzer and a 3.5-mm coaxial calibration standard (GCS35M). The far-field measurements were made in a full anechoic chamber with the dimensions of 15.2 m (W) × 7.9 m (L) × 7.9 m (H) at the RFID/USN Center, Incheon, Korea. The anechoic chamber can take far-field measurements ranging from 0.4 GHz to 18 GHz. When measuring the radiation pattern, a BBHA 9120 LFA broadband horn antenna was used for transmitting, while the proposed antenna was used for receiving. The transmitter and the receiver were separated by a distance of 9.6 m, while the proposed antenna was 0.5 m away from the positioner. The horn antenna was fixed, while the proposed dipole antenna loaded with SRRs was rotated from −180° to 180° at a scan angle of 1° and a speed of 3° s^{-1}.

Fig. 11 shows the measured and simulated reflection coefficients of the fabricated antenna. Minute disparities were seen between the measurements and the HFSS simulation, which could be associated with the misalignment in the fabrication procedures. As shown in Fig. 11, the measured impedance bandwidth at a reflection coefficient of less than −10 dB is 1.32–2.46 GHz (60.31%), while the simulated bandwidth is 1.38–2.41 GHz (54.35%).

The broadside gain and radiation patterns of the fabricated prototype at different frequencies were measured, and they are shown in Figs. 8 and 9, respectively. The antenna generates good broadside dipole-like radiation patterns, with a symmetrical profile and small fluctuations in gain within the entire impedance bandwidth. The radiation patterns are nearly constant

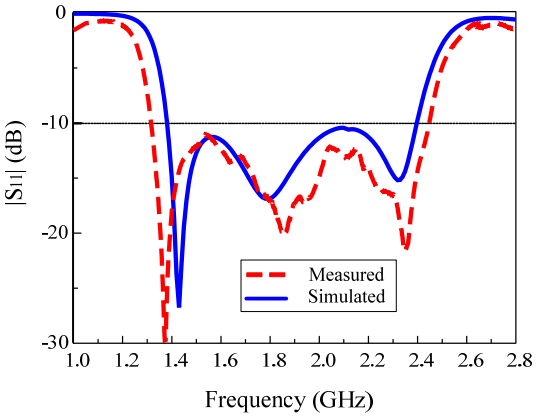

Fig. 11. Simulated and measured reflection coefficient values of the optimized dipole antenna loaded with SRRs.

and show a low cross-polarization level and little or no deterioration with increasing frequency. The radiation patterns are fairly symmetrical in both the xz- and yz-planes. The measurement results indicate some ripples in the radiation patterns. These ripples are attributed to the effects of the foam rack and tapes employed in the pattern measurement setup. At 1.42 GHz, the measurements showed a half-power beamwidth (HPBW) of 64.26° in the yz-plane and a broadside gain of 1.9 dBi. At 1.8 GHz, the prototype yielded a measured HPBW of 66.38° in the yz-plane and a broadside gain of 1.85 dBi. Further, at 2.33 GHz, the measurements indicated a HPBW of 54.48° in the yz-plane and a broadside gain of 2.0 dBi.

Fig. 8 compares the simulated and measured broadside gains of the fabricated antenna. The measurements indicated a peak gain of 2.1 dBi and high radiation efficiency of >88% across the operational bandwidth.

IV. Conclusion

A compact broadband composite dipole antenna with SRRs is presented. An analysis of the performance of the antennas with SRR splits at different locations is demonstrated. The antenna is capable of generating multi-resonances with a broad bandwidth. However, the bandwidth, number of generated resonances, and radiation pattern are influenced by the SRR split position. Therefore, the split position is a critical parameter in antenna design, because it has enormous effects on the antenna's major performance characteristics. The antenna demonstrated a broad bandwidth with stable dipole-like omnidirectional radiation patterns when SRR splits are at the optimum position.

This work was supported in part by the Institute for Information & Communications Technology Promotion grant funded by the Korean government (MSIP) (No. 2017-0-

00959, University ICT Basic Research Lab), in part by the "Human Resources Program in Energy Technology" of the Korean Institute of Energy Technology Evaluation and Planning granted financial resource from the Ministry of Trade, Industry & Energy, Republic of Korea (No. 2016-4030201380).

REFERENCES

[1] L. Wang, M. Q. Yuan, and Q. H. Liu, "A dual-band printed electrically small antenna covered by two capacitive split-ring resonators," *IEEE Antennas and Wireless Propagation Letters*, vol. 10, pp. 824–826, 2011.

[2] F. J. Herraiz-Martinez, L. E. Garcia-Munoz, D. Gonzalez-Ovejero, V. Gonzalez-Posadas, and D. Segovia-Vargas, "Dual-frequency printed dipole loaded with split ring resonators," *IEEE Antennas and Wireless Propagation Letters*, vol. 8, pp. 137–140, 2009.

[3] M. C. Tang and R. W. Ziolkowski, "A study of low-profile, broadside radiation, efficient electrically small antennas based on complementary split ring resonators," *IEEE Transactions on Antennas and Propagation*, vol. 61, no. 9, pp. 4419–4430, 2013.

[4] M. Li, X. Q. Lin, J. Y. Chin, R. Liu, and T. J. Cui, "A novel miniaturized printed planar antenna using split-ring resonator," *IEEE Antennas and Wireless Propagation Letters*, vol. 7, pp. 629–631, 2008.

[5] K. Xu, F. Liu, L. Peng, W. S. Zhao, L. Ran, and G. Wang, "Multimode and wideband printed loop antenna based on degraded split-ring resonators," *IEEE Access*, vol. 5, pp. 15561–15570, 2017.

[6] A. Erentok and R. W. Ziolkowski, "Metamaterial-inspired efficient electrically small antennas," *IEEE Transactions on Antennas and Propagation*, vol. 56, no. 3, pp. 691–707, 2008.

[7] J. B. Pendry, A. J. Holden, D. J. Robbins, and W. J. Stewart, "Magnetism from conductors and enhanced non-linear phenomena," *IEEE Transactions on Microwave Theory and Techniques*, vol. 47, no. 11, pp. 2075–2084, 1991.

[8] S. Zahertar, A. D. Yalcinkaya, and H. Torun, "Rectangular split-ring resonators with single-split and two-splits under different excitations and at microwave frequencies," *AIP Advances*, vol. 5, article no. 117220, 2015.

[9] P. Chen, L. Peng, A. Wu, and G. Wang, "Rendering wide impedance band of ESA made of SRRs," *Electronics Letters*, vol. 52, no. 19, pp. 1582–1584, 2016.

[10] J. P. Chen and P. Hsu, "A compact strip dipole coupled split-ring resonator antenna for RFID tags," *IEEE Transactions on Antennas and Propagation*, vol. 61, no. 11, pp. 5372–5376, 2013.

[11] E. Pucci, E. Rajo-Iglesias, M. N. M. Kehn, and O. Quevedo-Teruel, "Enhancing the efficiency of compact patch antennas composed of split-ring resonators by using lumped capacitors," *IEEE Antennas and Wireless Propagation Letters*, vol. 11, pp. 1362–1365, 2012.

[12] W. Cao, B. Zhang, A. Liu, T. Yu, D. Guo, and Y. Wei, "Gain enhancement for broadband periodic endfire antenna by using split-ring resonator structures," *IEEE Transactions on Antennas and Propagation*, vol. 60, no. 7, pp. 3513–3516, 2012.

[13] J. H. Kim and S. Nam, "A compact quasi-isotropic antenna based on folded split-ring resonators," *IEEE Antennas and Wireless Propagation Letters*, vol. 16, pp. 294–297, 2017.

[14] A. Dadgarpour, M. S. Sorkherizi, and A. A. Kishk, "A high-efficient circularly polarized magneto-electric dipole antenna for 5G applications using dual-polarized split-ring resonator lens," *IEEE Transactions on Antennas and Propagation*, vol. 65, no. 8, pp. 4263–4267, 2017.

[15] A. Habashi, J. Nourinia, and C. Ghobadi, "Mutual coupling reduction between very closely spaced patch antennas using low-profile folded split-ring resonators (FSRRs)," *IEEE Antennas and Wireless Propagation Letters*, vol. 10, pp. 862–865, 2011.

[16] K. E. Kedze, H. Wang, and I. Park, "Compact broadband omnidirectional radiation pattern printed dipole antenna incorporated with split-ring resonators," *IEEE Access*, vol. 6, pp. 49537–49545, 2018.

[17] S. X. Ta, I. Park, and R. W. Ziolkowski, "Broadband electrically small circularly polarized directive antenna," *IEEE Access*, vol. 5, pp. 14657–14663, 2017.

[18] H. H. Tran, S. X. Ta, and I. Park, "Single-feed, wideband, circularly polarized, crossed bowtie dipole antenna for global navigation satellite systems," *Journal of Electromagnetic Engineering and Science*, vol. 14, no. 3, pp. 299–305, 2014.

[19] S. X. Ta, J. J. Han, and I. Park, "Compact circularly polarized composite cavity-backed crossed dipole for GPS application," *Journal of Electromagnetic Engineering and Science*, vol. 13, no. 1, pp. 44–50, 013.

[20] K. E. Kedze, H. Wang, and I. Park, "Compact broadband dipole antenna with split-ring resonators," in *Proceedings of International Congress on Artificial Materials for Novel Wave Phenomena Metamaterials)*, Espoo, Finland, 2018, pp. 305–307.

Kam Eucharist Kedze

received his Bachelor of Technology in Electrical and Electronic Engineering (Telecommunication) degree from the University of Buea, Cameroon, in 2013. He is currently studying for his Ph.D. degree at the Department of Electrical and Computer Engineering at Ajou University, Suwon, Korea. His research interest is the design of patch antennas, crossed-dipole antennas, miniaturized antennas, and metasurface antennas.

Heesu Wang

received his B.S. degree in Electrical and Computer Engineering from Ajou University, Suwon, Korea, in 2018. He is currently studying for his M.S. degree at the Department of Electrical and Computer Engineering at Ajou University, Suwon, Korea. His research interest is the design of patch antenna, printed antennas, small antennas, and metasurface antennas for various wireless applications.

Ikmo Park

received the B.S. degree in Electrical Engineering from the State University of New York at Stony Brook and M.S. and Ph.D. degrees in Electrical Engineering from the University of Illinois at Urbana-Champaign. He joined the Department of Electrical and Computer Engineering at Ajou University, Suwon, Korea, in 1996. He has authored and co-authored over 300 technical journal and conference papers. He also holds over 40 domestic and international patents. He has served as a Chair of the Department of Electrical and Computer Engineering at Ajou University, and he is a member of the Board of Directors at the Korea Institute of Electromagnetic Engineering and Science (KIEES). He serves as the Editor-in-Chief for the Journal of KIEES, as an Editorial Board member for the *International Journal of Antennas and Propagation*, and as an Associate Editor for *IET Electronics Letters*. He has served as an Editorial Board member of the *Journal of Electromagnetic Engineering and Science*. He serves as chair, organizer, and member of program committees for various conferences, workshops, and short courses in electromagnetic-related topics. His current research interests include the design and analysis of microwave, millimeter-wave, terahertz wave, and nano-structured antennas with metamaterials and metasurfaces.